EUROPEAN ORGANIZATION FOR NUCLEAR RESEARCH

Proposal to the ISOLDE and Neutron Time-of-Flight Committee

Investigation of octupole deformation in neutron-rich actinium using high-resolution in-source laser spectroscopy

May 13, 2020

B. Andel[1], A. N. Andreyev[2], M. Au[3], A. E. Barzakh[4], A. J. Brinson[5], K. Chrysalidis[3], T. E. Cocolios[1], B. S. Cooper[6], J. Cubiss[2], H. De Witte[1], K. Dockx[1], D. V. Fedorov[4], V. N. Fedosseev[3], K. T. Flanagan[7], R. F. Garcia Ruiz[5], F. P. Gustafsson[1], R. Heinke[1], J. Johnson[1], M. Kadja[8], V. Leask[1,3], R. Lica[9], B. A. Marsh[3], P. L. Molkanov[4] G. Neyens[1,3], H. A. Perrett[7], S. Raeder[10], B. Reich[3], C. M. Ricketts[7], S. Rothe[3], M. D. Seliverstov[4], S. M. Udrescu[5], P. Van Duppen[1], A. R. Vernon[1], E. Verstraelen[1], K. Wendt[8], J. Wessolek[7], S. G. Wilkins[3], W. Wojtaczka[1], X. F. Yang[6]

[1] *KU Leuven, Belgium*
[2] *University of York, United Kingdom*
[3] *CERN EN-STI, Switzerland*
[4] *PNPI Gatchina, Russia*
[5] *Massachusetts Institute of Technology, United States*
[6] *Peking University, China*
[7] *The University of Manchester, United Kingdom*
[8] *Johannes Gutenberg University Mainz, Germany*
[9] *Horia Hulubei National Institute of Physics and Nuclear Engineering, Romania*
[10] *GSI Helmholtzzentrum für Schwerionenforschung, Germany*

Spokesperson: Reinhard Heinke (reinhard.heinke@cern.ch)
Contact person: Reinhard Heinke

CERN-INTC-2020-029 / INTC-P-556
13/05/2020

Abstract: We propose to perform high-resolution in-source laser spectroscopy measurements on the actinium isotopic chain $^{222-233}$Ac, to extract changes in mean-square charge radii as well as nuclear magnetic dipole and electric quadrupole moments with high precision. The results will pin down the border of octupole deformation in this part of the nuclear chart and validate state-of-the-art energy functional density calculations, incorporating reflection symmetry breaking. The measurements will be achieved by using a new operation mode of the LIST ion source.

Requested shifts: 19 shifts (1 run)

1 Introduction

Octupole collectivity, i.e. pear-shaped intrinsic configurations of nuclear ground states, have been prominently observed in the region around ^{222}Ra ($Z = 88$, $N = 134$) [1]. They are caused by strong correlations between nucleons in single-particle states of opposite parity near the Fermi surface, differing in three units of orbital and total angular momentum [2]. These systems with their breaking of reflection symmetry offer unique opportunities to study physics beyond the standard model, such as the search for permanent atomic electric dipole moments [3].
Recently, investigations in this part of the nuclear chart were extended to the neutron-rich side of the actinium isotopic chain. Nuclear ground state parameters were deduced by laser spectroscopy of hyperfine structure splittings and isotope shifts on $^{212-215,225-229}$Ac, including in-gas cell ($^{212-215}$Ac) [4] and high-resolution gas jet work (^{214,215}Ac) [5], high-resolution in-source data (^{225,227}Ac, to be published in [6], results already in [7]) and lower resolution in-source work at TRIUMF ($^{225-229}$Ac) [8, 7]. The results were compared to theoretical models [7]: The magnetic dipole moments can be explained by mixing of close-lying proton orbitals of opposite parity through an octupole field. Changes in mean-square charge radii were compared with different state-of-the-art energy density functional (EDF) calculations, where reflection symmetry breaking had to be incorporated [7].

2 Physics Interest

2.1 Changes in mean-square charge radii

An instructive picture of the present situation in the neutron-rich actinium region is given in Fig. 1a. The extracted changes in mean-square charge radii are compared to three different self-consistent EDF calculations, namely the DD-MEB2 [9] parametrization of a relativistic Lagrangian with density-dependent meson couplings, as well as the BSk31 [10] and SLy5s1 [11] parametrizations of the non-relativistic Skyrme force.
While the first two parametrizations are symmetry-restricted, the latter one allows for incorporation of reflection symmetry breaking, i.e. octupole deformation. On the neutron-rich side, the comparison shows an under- and overestimation, respectively, for the BSk31 and DD-MEB2 calculations, while SLy5s1 reproduces the experimental values best. On the neutron-deficient side below the $N = 126$ shell closure, all calculations perform similarly. The SLy5s1 calculations were carried out with and without forced reflection symmetry, strongly hinting to the necessity of incorporating the octupole degree of freedom to reproduce the experimental values (Fig. 1b). Here, the region where octupole deformation is expected to be present in the actinium isotopes is evidently shown as well: Starting at $N = 131$ (^{220}Ac), the trend continues up to ^{228}Ac, gets less pronounced from there on and vanishes again in the transition over $^{230-232}$Ac, i.e. $N = 141$ - 143. It will be extremely valuable to trace the evolution of the mean-square charge radii along the neutron-rich end to pin down the onset of octupole correlation in the ground state of these nuclei. The pronounced "kink" at $N = 141$ will enable us to confidently validate the applicability of the model, and thus the occurrence of reflection-symmetry breaking in this region. Expansion to the onset point at lower masses (around $N = 131$) is out of reach from an

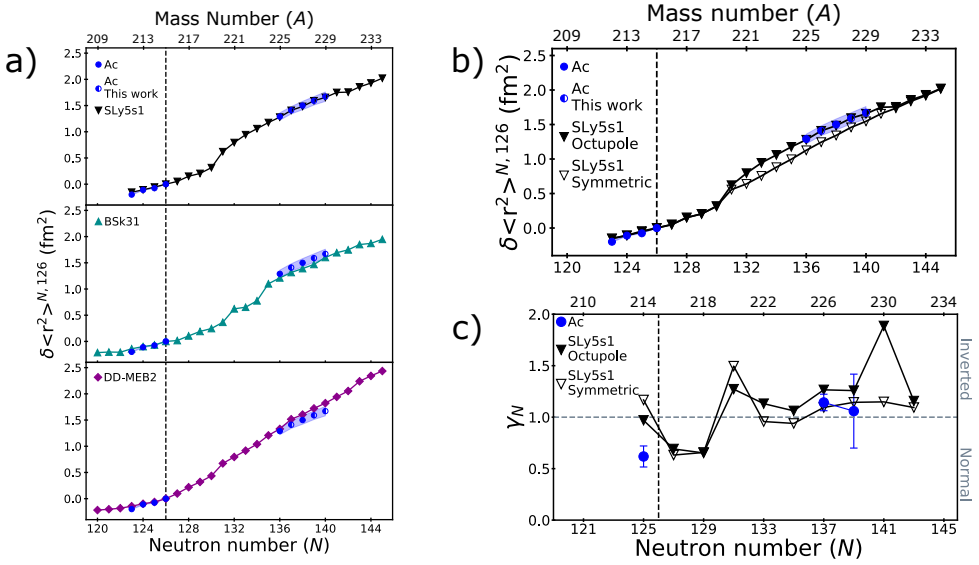

Figure 1: (a) Comparison of experimental changes in mean-square charge radii $\delta\langle r^2\rangle^{N,126}$ with different EDF calculations as described in the text. (b) SLy5s1 calculations with and without forced reflection symmetry. (c) Comparison of the staggering parameter γ_N with predictions from the SLy5s1 calculations. A precise measurement at $N = 139$ will pin down the range of inverted staggering, with $N = 141$ being a powerful case to discriminate the models. All figures adapted from [7].

isotope production point of view.

Reversed odd-even staggering in the charge radii in this region has been associated with reflection asymmetry for different elements, for example polonium [12], astatine [13], francium [14] and radium [15] - however, its direct link is disputed [2, 16, 7]. Finally, odd-even staggering has recently been highlighted as a particularly sensitive observable for state-of-the-art nuclear models [17]. The staggering parameter, γ_N, as introduced by [18] is shown in Fig. 1c for experimental values and those calculated from the two SLy5s1 variants.

At $N = 139$, inverted odd-even staggering ($\gamma_N > 1$) vanishes for the radium and francium isotopes [7], which could not be confirmed for the actinium chain due to the large uncertainty in the experimental data. Enhanced spectral resolution in measurements of $^{227-229}$Ac beyond the Doppler limitation in hot cavity ion sources is crucial to determine this point. The extreme predicted value for ^{230}Ac is directly linked to the disappearance of octupole deformation at $N = 142$, and a measurement of this value provides a sensitive probe to differentiate between the restricted and unrestricted SLy5s1 calculations. On the more neutron-deficient side ($N < 137$), the respective models can also be tested over an extended range. Especially the "step" predicted by BSk31 between ^{222}Ac and ^{223}Ac (Fig. 1a) can be probed.

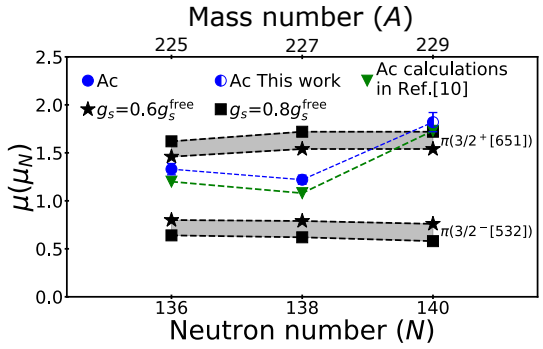

Figure 2: Comparison of magnetic dipole moments with theoretical values of indicated pure orbitals. The values of ^{225,227}Ac can be explained by mixing of the states, implying octupole collectivity, while at ^{229}Ac this effect strongly decreases. See text for detailed description. Figure adapted from [7].

2.2 Nuclear moments

Octupole collectivity can also be investigated by comparing experimental nuclear magnetic moments, μ, with theoretical values for pure single nucleon orbitals. Nuclear magnetic dipole and electric quadrupole moments can be deduced from the hyperfine splitting (HFS) parameters A and B, as described for example in [19]. The magnetic moments for ^{225,227,229}Ac were compared in [7] to theoretical values of the low-lying, near-degenerate and opposite-parity $\pi(3/2^-\ [532])$ and $\pi(3/2^+\ [651])$ orbitals as shown in Fig. 2.
The theoretical values were calculated with input from [20, 21, 22], suggesting g_s values ranging from 0.6 to 0.8 g_s^{free} as shown in the figure. For ^{225,227}Ac, the experimental values lie in between, thus requiring mixing of both opposite-parity states as implication of octupole collectivity. ^{229}Ac in contrast coincides with the $\pi(3/2^+\ [651])$ orbital value, thus implying a significant decrease in the influence of the octupole degree of freedom with increasing neutron number. Also in this case, extending the measurements to heavier isotopes will allow the upper border of reflection asymmetry to be ascertained. Dipole moment calculations in [23], using an octupole-deformed Woods-Saxon model with a reflection asymmetric rotor (shown as green triangles in Fig. 2), also reproduce the trend of the measured values, albeit systematically shifted to lower values. This also gives confidence in the octupole deformation explanation approach, and here, once again, ^{229}Ac is shown to be just at the border of this range. Additionally, more accurate data from high resolution measurements on ^{226,228}Ac is needed to draw definite conclusions on their octupolarity, as on the present state the interpretation in the additivity relation framework remains ambiguous [7]. Furthermore, clear assignment of nuclear spins requires full resolution of the individual hyperfine structure, as ^{226,229}Ac are tentatively determined by the splitting of the excited atomic state only [7].
The disentanglement of contributions from quadrupole and octupole deformation on the structure effects is not possible without taking other observables into account. The spectroscopic electric quadrupole moment Q_s, exhibiting only minor contributions to the hyperfine structure, becomes accessible only in spectroscopy methods with resolution beyond hot cavity Doppler limitations. As already performed for ^{225,227}Ac [6, 7] and ^{214,215}Ac [5], we will extract these values for the remaining isotopes with sufficient yield (^{224,226,228}Ac) as additional test parameter for theoretical models.
The unambiguous assignment of hyperfine A and B parameters to both electronic states involved in the spectroscopic investigation will lastly allow us to track possible hyperfine anomalies via the ratio of the A parameters along the isotopic chain. An influence of

octupolarity is expected (due to similarities in its operator to the magnetic moment operator), but has so far never been investigated.

3 Method: RILIS/PI-LIST in-source spectroscopy

The resonance ionization laser ion source (RILIS) has been proven to be a powerful tool for laser spectroscopy measurements of nuclear parameters with unrivaled sensitivity [24]. The results presented in the previous section have been achieved with a well-established two-step resonance ionization scheme (Fig. 3a) developed in [25, 26, 27]. It was recently used for yield and release studies [28] and implantation of ^{229}Ac [29] at ISOLDE . With standard in-source resolution, only the hyperfine splitting of the excited state can be resolved. The smaller splitting in the ground state prevents single resonance line allocation in the Doppler-broadened hot-cavity environment. The transition isotope shifts of typically a few GHz per mass unit can be resolved.

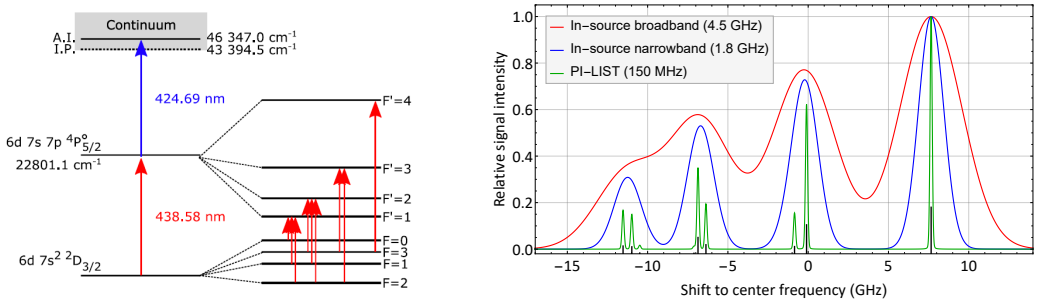

(a) (b)

Figure 3: (a) Resonance ionization laser scheme for actinium, taken from [7]. (b) Calculated experimental resolution (convoluted laser bandwidth and Doppler broadening at 2000 °C) on ^{227}Ac for different operation modes, scaled to respective maximum. Position and theoretical relative intensities of the resonances are shown as black bars. The red line resembles the resolution achieved at TRIUMF [7, 8], the blue line the achievable resolution with 1 GHz FWHM laser bandwidth under the same conditions. The green line illustrates the possibility to disentangle the ground state splitting, based on [6], with the PI-LIST. While the first two can be comparable in efficiency, a loss factor of 10^3 can be expected when switching to PI-LIST mode.

Detection of the ionization rate with respect to the laser frequency can be carried out with single ion counting (MagneToF detector at CA0) for the abundantly produced and longer-lived $^{224-229}$Ac isotopes. For the α- and β-emitters on the more neutron-deficient and neutron-rich sides, respectively, we will use the ISOLDE Decay Station (IDS) with a fast movable tape implantation point with an annular Si detector in front and plastic scintillators behind. In-source spectroscopy performed at ISOLDE using RILIS combined with established nuclear decay detection methods, including IDS, has been very productive in recent years [30]. Sensitivity down to less than 0.1 ion/s has been demonstrated [31, 32]. In order to measure hyperfine coupling constants and isotope shifts with sufficient precision in extraction of spectroscopic quadrupole moments and unambiguously determine the

odd-even staggering behavior, we propose application of the *Perpendicularly Illuminated Laser Ion Source and Trap* PI-LIST. It is based on the standard ISOLDE LIST laser ion source for production of clean beams, that was employed for polonium [12] and recently for magnesium [33]. The upgrade enables perpendicular laser irradiation inside the LIST's RFQ structure, circumventing Doppler broadening restrictions in the hot atomic vapor [34]. Its capability to reach experimental linewidths down to 100 - 200 MHz has been documented in various off-line experiments [34, 35, 36, 6]. Projected experimental data quality is shown in Fig. 3b. The increase in resolution is accompanied by a decrease in ionization efficiency by roughly a factor of not more than 10^3 compared to standard RILIS geometry [36]. A suitable narrow-bandwidth laser system and expertise in high-resolution, high-stability laser spectroscopy are available in cooperation between RILIS and CRIS as demonstrated in [37], where continuous wave laser light from the CRIS laboratory was used as the seed for a single-mode pulsed amplification stage in the RILIS setup. The PI-LIST will be used on-line in the approved IS456 experiment on polonium [38], where its performance will be validated. Measurements on the isotopes with lower yields ($^{222-223,230-233}$Ac) can be performed in standard LIST mode (resembling RILIS), allowing deduction of the changes in mean-square charge radii on at least the same quality level as in [7], before potentially changing to high resolution mode.

Target and yields: We propose a UC target as used for previous actinium production. Yields were extracted during [28] for $^{224-231}$Ac, and estimations for ^{222,223,232,233}Ac are inferred from half-life behavior and FLUKA calculations. A summary is given in Tab. 1.

Summary of requested shifts: Tab. 1 gives a summary of the requested **19 shifts**.

Table 1: Actinium yields inferred from [28], and intended measurements (isotope shifts (IS), magnetic dipole (μ) and electric quadrupole (Q_s) moments), with values known from literature in brackets. 1000-fold reduced yield is given for PI-LIST high resolution application, and 30-fold reduction for LIST to suppress surface-ionized Ra and Fr.

Isotope	$T_{1/2}$	Yield (ions/μC)			Det.	Measurement	Shifts
		RILIS	LIST	PI-LIST			
^{222}Ac	63 s	2	0.1		α	IS, μ	2
^{223}Ac	2.10 min	1×10^3	30		α	IS, μ	2
^{224}Ac	2.78 h	9×10^5		9×10^2	ions	IS, μ, Q_s	1
^{225}Ac	9.92 d	3×10^7		3×10^4	ions	**Ref.**	0.5
^{226}Ac	29.37 h	3×10^6		3×10^3	ions	(IS, μ), Q_s	0.5
^{227}Ac	21.77 y	3×10^7		3×10^4	ions	**Ref. & Setup**	1.5
^{228}Ac	6.15 h	2×10^6		2×10^3	ions	(IS, μ), Q_s	0.5
^{229}Ac	62.7 min	3×10^5		3×10^2	ions/β	(IS, μ), Q_s	1
^{230}Ac	122 s	3×10^2	10		β	IS, μ	2.5
^{231}Ac	7.5 min	2×10^3	70		β	IS, μ	2.5
^{232}Ac	1.98 min	80	3		β	IS, μ	2.5
^{233}Ac	145 s	70	2		β	IS, μ	2.5
Total:							**19**

References

[1] L. P. Gaffney, *et al.*, *Nature* **497**(7448), 199 (2013).

[2] P. A. Butler, W. Nazarewicz, *Reviews of Modern Physics* **68**(2), 349 (1996).

[3] R. F. Garcia Ruiz, *et al.*, *Nature* **(accepted)** (2020).

[4] C. Granados, *et al.*, *Physical Review C* **96**(5), 054331 (2017).

[5] R. Ferrer, *et al.*, *Nature communications* **8**, 14520 (2017).

[6] S. Raeder, *et al.*, *To be published* .

[7] E. Verstraelen, *et al.*, *Physical Review C* **100**(4), 044321 (2019).

[8] A. Teigelhöfer, *Isotope shift and hyperfine structure measurements on silver, actinium and astatine by in-source resonant ionization laser spectroscopy*, Phd thesis, The University of Manitoba (2017).

[9] D. Peña-Arteaga, S. Goriely, N. Chamel, *The European Physical Journal A* **52**(10), 320 (2016).

[10] S. Goriely, N. Chamel, J. M. Pearson, *Physical Review C* **93**(3), 034337 (2016).

[11] R. Jodon, M. Bender, K. Bennaceur, J. Meyer, *Physical Review C* **94**(2), 024335 (2016).

[12] D. A. Fink, *et al.*, *Physical Review X* **5**(1), 011018 (2015).

[13] A. E. Barzakh, *et al.*, *Physical Review C* **99**(5), 257 (2019).

[14] I. Budinčević, *et al.*, *Physical Review C* **90**(1), 014317 (2014).

[15] K. M. Lynch, *et al.*, *Physical Review C* **97**(2), 024309 (2018).

[16] H. Iimura, F. Buchinger, *Physical Review C* **78**(6), 067301 (2008).

[17] R. P. de Groote, *et al.*, *Nature Physics* (2020).

[18] W. J. Tomlinson, H. H. Stroke, *Nuclear Physics* **60**(4), 614 (1964).

[19] P. Campbell, I. D. Moore, M. R. Pearson, *Progress in Particle and Nuclear Physics* **86**, 127 (2016).

[20] C. Ekström, L. Robertsson, A. Rosén, *Physica Scripta* **34**(6A), 624 (1986).

[21] R. Neugart, G. Neyens, in J. Al-Khalili E. Roeckl (eds.), *The Euroschool Lectures on Physics with Exotic Beams, Vol. II*, vol. 700 of *Lecture Notes in Physics*, pp. 135–189. Springer Berlin Heidelberg (2006).

[22] R. K. Sheline, G. A. Leander, *Physical Review Letters* **51**(5), 359 (1983).

[23] Leander, Chen, *Physical review. C, Nuclear physics* **37**(6), 2744 (1988).

[24] V. Fedosseev, *et al.*, *Journal of Physics G: Nuclear and Particle Physics* **44**(8), 084006 (2017).

[25] J. Roßnagel, *et al.*, *Physical Review A* **85**(1), 1478 (2012).

[26] S. Raeder, *et al.*, *Hyperfine Interactions* **216**(1-3), 33 (2013).

[27] S. Raeder, *et al.*, *Nuclear Instruments and Methods in Physics Research Section B: Beam Interactions with Materials and Atoms* **376**, 382 (2016).

[28] K. Dockx, *et al.*, 'Towards reliable production of 225Ac for medical applications: Systematic analysis of the production of Fr, Ra and Ac beams.', Tech. Rep. CERN-INTC-2017-016. INTC-P-498, CERN, Geneva (2017).

[29] M. Verlinde, *et al.*, *Physical Review C* **100**(2), 024315 (2019).

[30] A. Andreyev, *et al.*, 'Shape-coexistence and shape-evolution studies for bismuth isotopes by in-source laser spectroscopy ', Tech. Rep. CERN-INTC-2017-005. INTC-P-443-ADD-1, CERN, Geneva (2017).

[31] T. E. Cocolios, *et al.*, *Physical review letters* **106**(5), 052503 (2011).

[32] B. A. Marsh, *et al.*, *Nature Physics* **14**(12), 1163 (2018).

[33] B. Blank, *et al.*, 'Measurement of the super-allowed branching ratio of ^{22}Mg', Tech. Rep. CERN-INTC-2016-010. INTC-P-459, CERN, Geneva (2016).

[34] R. Heinke, *et al.*, *Hyperfine Interactions* **238**(1), 127 (2017).

[35] D. Studer, *et al.*, *The European Physical Journal A* **56**(2), 127 (2020).

[36] R. M. Heinke, *In-source high-resolution spectroscopy of holmium radioisotopes - Online tailored perpendicular laser interaction at ISOLDE's Laser Ion Source and Trap LIST*, Phd thesis, Johannes Gutenberg University Mainz, Mainz (2019).

[37] K. Chrysalidis, *et al.*, *Nuclear Instruments and Methods in Physics Research Section B: Beam Interactions with Materials and Atoms* **463**, 476 (2020).

[38] A. Andreyev, A. Barzakh, T. E. Cocolios, B. Marsh, R. Lica, 'IS456 - Study of polonium isotopes ground-state properties by simultaneous atomic and nuclear spectroscopy', Tech. Rep. CERN-INTC-2019-032. INTC-SR-089, CERN, Geneva (2019).

Appendix

DESCRIPTION OF THE PROPOSED EXPERIMENT
The experimental setup comprises: (*name the fixed-ISOLDE installations, as well as flexible elements of the experiment*)

Part of the	Availability	Design and manufacturing
IDS	☒ Existing	To be modified: Addition of annular Si detector for α decay spectroscopy
RILIS + CRIS narrow band	☒ Existing	To be used without modification

HAZARDS GENERATED BY THE EXPERIMENT (if using fixed installation:) Hazards named in the document relevant for the fixed [COLLAPS, CRIS, ISOLTRAP, MINIBALL + only CD, MINIBALL + T-REX, NICOLE, SSP-GLM chamber, SSP-GHM chamber, or WITCH] installation: **No additional hazards.**

Average electrical power requirements (excluding fixed ISOLDE-installation mentioned above): **No additional requirements.**